Laser Review

Recent Advances in Trace Gas Detection Using Quantum and Interband Cascade Lasers

Frank K. TITTEL, Yury BAKHIRKIN, Anatoliy A. KOSTEREV and Gerard WYSOCKI
Rice Quantum Institute, Rice University, Houston, TX 77251-1892, USA

(Received January 17, 2006)

There is an increasing need in many chemical sensing applications ranging from environmental science to industrial process control as well as medical diagnostics for fast, sensitive, and selective trace gas detection based on laser spectroscopy. The recent availability of novel pulsed and continuous wave (cw) quantum and interband cascade distributed feedback (QC and IC DFB) lasers as mid-infrared spectroscopic sources addresses this need. A number of spectroscopic techniques have been demonstrated worldwide. For example, the authors have employed infrared DFB QC and IC lasers for the detection and quantification of trace gases and isotopic species in ambient air at ppmv, ppbv and even sub-ppbv levels by means of direct absorption, cavity enhanced, photoacoustic and wavelength modulation spectroscopy.

Key Words: Chemical sensing of trace gases, Quantum and interband cascade lasers, Infrared absorption spectroscopy, Photoacoustic spectroscopy techniques, Cavity enhanced absorption spectroscopy

1. Introduction

Infrared laser absorption spectroscopy is an extremely effective tool for the detection of molecular trace gases. The demonstrated sensitivity of this technique ranges from parts per million by volume (ppmv) to the parts per trillion (pptv) level depending on the specific gas species.[1,2] The usefulness of the laser spectroscopy approach is limited by the availability of convenient tunable sources in the region of fundamental vibrational absorption bands from 3 to 24 μm. Real world applications (see Table 1) require the laser source to be compact, efficient, reliable and operating at near room-temperatures. Existing options include lead salt diode lasers, coherent sources based on difference frequency generation (DFG), optical parametric oscillators (OPOs), tunable solid state lasers, quantum and interband cascade lasers. Sensors based upon lead salt diode lasers are typically large in size and require cryogenic cooling because these lasers operate at temperatures of < 90 ˚K. DFG based sources (especially bulk and waveguide PPLN based) have been shown to be robust and compact.[3,4] The recent advances of quantum cascade (QC) and interband cascade (IC) lasers fabricated by band structure engineering offer an attractive new source option for infrared absorption spectroscopy with ultra-high resolution and sensitivity.[5] The most technologically developed mid-infrared QC laser source to date is based on type-I intersubband transitions in InGaAs/InAlAs heterostructures.[6-11] More recently interband cascade lasers (ICLs) based on type-II interband transition have been reported in the 3 - 5 μm region.[12-14] Other potential QCLs based on GaAs/AlGaAs material system were reported as well.[15,16]

Table 1 Wide range of gas sensing applications.

Urban and Industrial Emission Measurements
Industrial Plants
Combustion Sources and Processes (e.g. early fire detection)
Automobile and Aircraft Emissions
Rural Emission Measurements
Agriculture and Animal Facilities
Environmental Gas Monitoring
Atmospheric Chemistry (e.g. ecosystems and airborne)
Volcanic Emissions
Chemical Analysis and Industrial Process Control
Chemical, Pharmaceutical, Food & Semiconductor Industry
Toxic Industrial Chemical Detection
Spacecraft and Planetary Surface Monitoring
Crew Health Maintenance & Advanced Human Life Support Technology
Biomedical and Clinical Diagnostics (e.g. breath analysis)
Forensic Science and Security
Fundamental Science and Photochemistry

DFB-QC lasers allow the realization of compact, narrow linewidth, mid-IR sources combining single-frequency operation and substantially high powers (tens of mW) at mid-IR wavelengths (4 to 24 μm) at temperatures attainable with thermoelectric cooling. The large wavelength coverage available with QC lasers allows identification, detection, quantification and monitoring of numerous molecular trace gas species, especially those with resolved rotational-vibrational spectra. The high QC laser output power permits the use of advanced detection techniques that significantly improve the detection sensitivity of trace gas species and decrease the complexity and size of the overall sensor architecture. For example, in Integrated Cavity Output Spectroscopy (ICOS) and Cavity Ringdown Spectroscopy (CRDS) an effective absorption pathlength of hundreds of meters can be obtained in a laptop-size device.[17]

Unipolar DFB-QC lasers are inherently capable of operating at high temperature of the active region, considerably exceeding room temperature. However, the power dissipation in these devices is higher than in bipolar diode lasers and often surpasses 10 W. Until 2004, it was not possible to realize cw operation of QC lasers without cryogenic cooling. For example, a cw DFB-

QC laser operated at 82 ˚K in a liquid nitrogen Dewar was used in an airborne sensor for atmospheric detection of CH_4 and N_2O.[18] The cw QC-DFB laser linewidth is < 1 MHz when a ripple-free current source is used[19] and can be a few 100's Hz when frequency stabilization feedback is employed.[20]

An effective practical solution for non-cryogenic DFB-QC laser based spectroscopy is to apply very short (5-50 ns) pump current pulses at a low duty cycle, typically < 1 %. In pulsed operation the minimum DFB-QC laser linewidth is typically ~ 150-350 MHz due to the frequency chirp related to the fast heating of the active area during the pump current pulse.[21] Gas concentration measurements are usually performed either at pressures of ~ 100 Torr or at atmospheric pressures where pressure broadened absorption lines are ~ 3 GHz. Hence the pulsed mode of DFB-QC laser operation has a clear advantage for compact field deployable sensors because it eliminates the need for cryogenic cooling. However, recent progress in the development of both cw thermoelectrically cooled Fabry-Perot and DFB QC lasers[22,23] significantly facilitates the design of chemical sensors based on QCL technology. In addition, thermoelectrically cooled Fabry-Perot QC lasers have been used in widely tunable grating coupled cavity configurations.[24-26]

2. Chemical sensing based on direct IR absorption spectroscopy

2.1 Detection of trace gases with pulsed DFB QC lasers

The first work on spectroscopic chemical sensing with a pulsed QC-DFB laser was reported in 1998. A technique of fast-tuning the optical frequency of the laser pulses by applying a subthreshold current (STC) ramp was introduced.[21,27] This approach uses short duration current pulses of 5 to 25 nsec, which are tuned through an absorption feature by use of a subthreshold current ramp. Wavelength modulation (WM) spectra of diluted N_2O and CH_4 samples were acquired near $\lambda = 8$ μm. A similar approach to detection was used in Ref. 28 and referred to as "quasi-cw".

An alternative approach to data acquisition with pulsed DFB-QC lasers is to use a fast detector and measure peak power of every pulse with gated electronics. In this mode of measurement the detected signal is much higher than the detector noise and does not depend on the repetition rate. Time-gating permits suppression of the scattered light that occurs earlier or later than the informative signal. This approach was utilized in the application of a pulsed DFB-QC laser to trace gas detection in ambient air.[27] Another method relies on the linear frequency chirp obtained from a QC laser when relatively long (> 100 ns) current pulses are applied to map the spectral information into the temporal domain.[29] This approach requires an IR detector and a an analog digital converter (ADC) with a temporal resolution of ~ 1 ns or better. The ultimate spectral resolution is given by the equation $\Delta\nu = C(d\nu/dt)^{1/2}$, where C~1 is a dimensionless constant and dn/dt is the chirp rate.[30]

A schematic of a typical pulsed QC-DFB laser based gas sensor configuration used by the authors is shown in Fig. 1. A DFB QC laser designed for pulsed near-room temperature operation is mounted on a thermoelectric cooling module inside a compact evacuated housing. The temperature of the DFB QC laser can be varied from - 40 ˚C to above room temperature. In practice, the laser temperature is usually kept < 6 ˚C because of a rapid decrease in laser power, an increase of threshold current and the appearance of mode instabilities at higher temperatures.

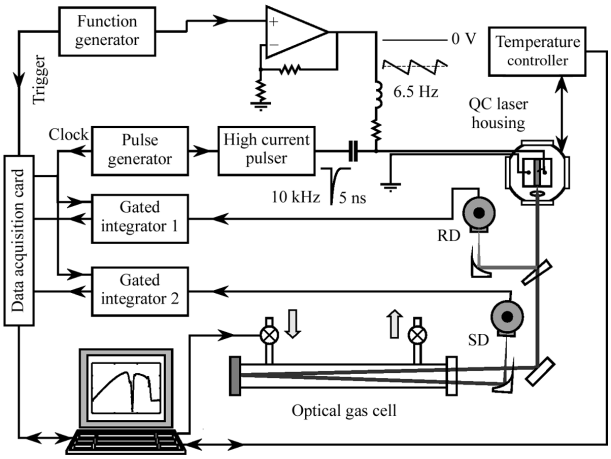

Fig. 1 Schematic of a pulsed thermo-electric cooled DFB QC-laser based gas sensor.[33]

The laser is pumped by 5 ns long current pulses at repetition rates up to 1 MHz. Such short pulses resulted in a minimum QC laser linewidth, typically 290 MHz. A novel approach for wavelength manipulation of the DFB-QCL pulses is used. A STC waveform is synthesized by a computer-controlled digital-analogue converter (DAC) or a ramp from an external function generator. The timing of consecutive STC updates was synchronized to the pump current pulses. In this manner, the relative wavelength of each laser pulse in a wavelength scan can be independently and unambiguously controlled. Computer control adds practical flexibility to the QC laser based sensor architecture. The laser pulses can be detected using either a liquid nitrogen cooled or a thermoelectrically cooled HgCdTe (MCT) detector. For data analysis a linear regression technique similar to the one first developed in Ref. 31 for ethanol detection was used. This technique is applied to perform the concentration calculations and takes into account a non-negligible asymmetric laser line shape. The flexibility provided by the digital frequency control approach was also utilized for linearization of the wavelength scan and for wavelength modulation spectroscopy.

Specific examples of trace gas detection based on thermoelectrically cooled pulsed DFB quantum cascade lasers follow:

2.1.1 $^{13}CO_2/^{12}CO_2$ isotopic ratio measurements at 4.3 μm

A field-deployable, pulsed quantum cascade laser spectrometer was reported in Ref 32. An instrument was designed to measure the $^{13}C/^{12}C$ isotopic ratio in the CO_2 released from volcanic vents. Specific $^{12}CO_2$ and $^{13}CO_2$ absorption lines were selected around 4.3 μm, where the P-branch of $^{12}CO_2$ overlaps the R-branch of $^{13}CO_2$ of the 0001–0000 vibrational transition. This particular selection makes the instrument insensitive to temperature variations. A dual-channel cell balances the two absorption signals. The basic sensor concept was demonstrated by measuring $^{16}O^{12}C^{16}O$ and $^{16}O^{12}C^{18}O$ concentrations in a 1 % CO_2 mixture in N_2 in the spectral region of 2320 cm^{-1}.

2.1.2 Ambient atmospheric carbon monoxide monitoring at 4.6 μm

Carbon monoxide (CO) is a pollutant produced by the incomplete combustion of carbon-based fuels that are widely used for power generation, industrial heating, petrochemical refining, and propulsion. The current US EPA-approved method for continuous monitoring of ambient CO is non-dispersive infrared (NDIR) technology, which is generally limited in sensitivity to > 1 ppm,

requires sample gas pre-treatment, suffer from the potential of interfering non target gas species and has response times on the order of 30 s. QC laser based CO sensors with < 100 ppb detection sensitivity in 1 sec now offer an attractive alternative for effective apportionment and control of CO emissions.

A pulsed, thermoelectrically cooled QC-DFB laser operating at 4.6 μm[33] was used to probe isolated absorption transitions in the fundamental CO vibrational band. The QC-DFB laser was operated according to the procedures described in Ref. 27. The DFB QC laser was excited by ~ 5 ns long, ~ 2 A peak current pulses at a repetition rate of 10 kHz. A sawtooth-modulated sub-threshold current was added to the excitation pulses in order to tune the laser wavelength. The modulation frequency was set to 6.5 Hz so that ~ 1500 laser pulses were generated during one period. With the appropriate settings of the QC laser temperature and current, the laser frequency could be tuned over a 0.41 cm^{-1} region encompassing the R(3) absorption line at 2158.3 cm^{-1}. This transition is interference free from atmospheric species such as H_2O and CO_2. The laser frequency scan was calibrated using interference fringes from an uncoated ZnSe air-gap etalon with a FSR of 0.03 cm^{-1}. Absolute frequency assignment was performed by comparison of experimental absorption spectra of CO and N_2O with the HITRAN 2000 database.[34]

The peak intensity of each pulse was measured using two gated integrators (one for each detector) with an integration window set to ~15 ns, and subsequently digitized with a 16 bit data acquisition card (National Instruments DAQCard-AI-16XE-50). Air was automatically sampled in the gas cell via a computer-controlled valve and a pressure controller that ensured constant pressure of 95 Torr during the data acquisition process. The laser line was found to have an asymmetric shape and a FWHM of ~ 0.02 cm^{-1} comparable to the CO absorption line width of 0.018 cm^{-1} at 95 Torr air pressure. To extract the CO concentration from the spectral data we used the same procedure as described in Ref. 35 .

An example CO absorption spectrum acquired using 500 laser sweep averages for each of an evacuated and air-filled measurement is shown in Fig. 2 (a) along with the best-fit line. From the fit residual shown in Fig. 2 (b) the single-point standard deviation of the measured fractional absorbance is $\sigma = 1.5 \times 10^{-4}$. For a pathlength of 102 cm and the selected CO absorption line, this translates into a noise-equivalent detection limit of δ[CO] = 6.5 ppb.

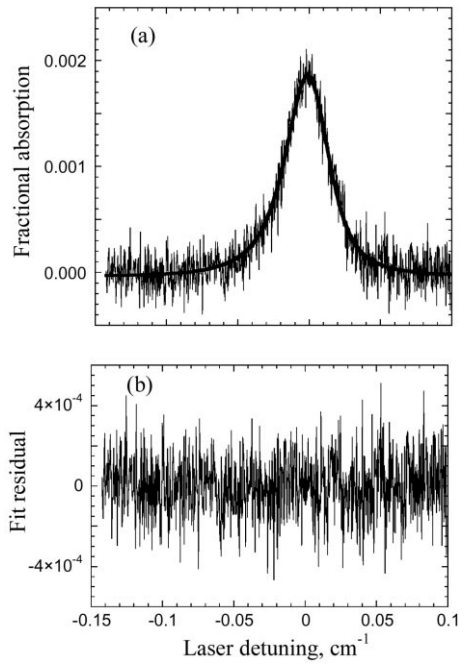

Fig. 2 (a) Typical example of CO absorption detected in ambient air; (b) fit residual.

The CO sensor was also applied to continuous monitoring of the CO concentration in ambient laboratory air detected by its R(3) absorption line. A noise-equivalent detection limit of 12 ppbv was obtained with a 1 m optical pathlength and a 2.5 min data acquisition time. This sensitivity corresponds to a standard error in fractional absorbance of 3×10^{-5}. Two characteristic maxima of CO concentration were observed during a typical day, corresponding to morning and evening rush hour traffic on a street adjacent to the Rice University campus as evident in Fig. 3.[33] The short duration behavior of these broad maxima, however, was closely connected with local meteorological conditions such as wind.

2.1.3 Nitric oxide detection at 5.2 μm

Detection of nitric oxide (NO) is important in many applications that include industrial emission and process monitoring[36] atmospheric research,[37] and medical diagnostics.[38,39] In recent years stricter regulatory limits for the maximum allowable concentrations of toxic pollutants in industrial exhaust gases were imposed. This triggered a need for sensors capable of real-time concentration monitoring of NO at parts per million (ppmv) levels to ensure regulatory compliance. An instrument suitable for direct *in situ* spectroscopic analysis of industrial exhaust gases must address specific environmental challenges including atmospheric analyte gas pressure, strong nonselective absorption by soot particles, high temperature, and overlapping absorption lines of different gas species.[40]

Nelson et al.[41] reported measurements of nitric oxide in air with a detection limit of less than 1 nmole/mole (< 1 ppbv) using a thermoelectrically cooled quantum cascade laser operated in a pulsed mode at 5.26 μm (1897 cm^{-1}) and coupled to a 210-m path length multiple-pass absorption cell at a reduced pressure (50 Torr). The sensitivity of the system is enhanced by operating under pulsing conditions which reduce the laser line

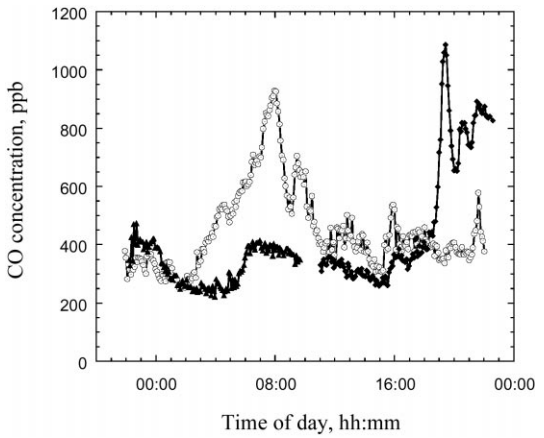

Fig. 3 Three test runs of continuous CO monitoring in ambient laboratory air.[27] These test runs started on Friday, 9 March, 2001 (diamonds), on Tuesday, 13 March, 2001 (open circles) and on 14 March, 2001 (triangles) respectively. Interval between consecutive measurements was 5 min.

width to 0.01 cm^{-1} (300 MHz) HWHM, and by normalizing pulse-to-pulse intensity variations with temporal gating on a single HgCdTe detector. A detection precision of 0.12 ppb $Hz^{-1/2}$ is achieved with a liquid-nitrogen-cooled detector. This detection precision corresponds to an absorbance precision of 1 $\times 10^{-5}$ $Hz^{-1/2}$ or an absorbance precision per unit path length of 5 $\times 10^{-10}$ $cm^{-1}Hz^{-1/2}$.

2.1.4 Ammonia detection at 10 μm

High sensitivity detection of NH_3 is of significant interest in the control of the NO_x chemistry, industrial safety and medical diagnostics, especially for kidney related diseases and therapy. A compact transportable ammonia sensor based on a thermoelectrically cooled pulsed QC-DFB laser operating at ~ 10 microns was described in Ref. 35. The laser was scanned over two absorption lines of the NH_3 fundamental ν_2 band. This sensor was successfully applied to continuous long-term monitoring of NH_3 concentration levels present in bioreactor vent gases at the NASA Johnson Space Center, Houston, TX,. A sensitivity of better than 0.3 ppmv was achieved with a 1 m optical pathlength, which was sufficient to quantify expected dynamic ammonia levels of 1 to 10 ppmv.

2.2 Detection of trace gases with CW QC-DFB lasers

Gas sensing with a cw DFB QC laser was first reported in Ref. 42 .

2.2.1 CH_4 and N_2O detection at 7.9 μm

The direct absorption approach with cw QC-DFB lasers was further developed[43] and the first successful application of a single-frequency DFB-QC laser to the analysis of trace gases in ambient air was reported in Ref. 31. In these experiments, a DFB-QC laser designed for cw operation at cryogenic temperatures in the 7.9 μm spectral region was used. To avoid fast boil-off of liquid nitrogen and related frequency and alignment drifts, the laser was operated at a reduced duty cycle (typically 10 % to 25 %). Current was supplied in pulses of 120 to 235 μs duration at a 0.8 to 1 KHz repetition rate. The lasing characteristics under such long pump current pulses are essentially the same as in real cw operation, because the temperature of the laser active region reaches equilibrium on a nanosecond time scale. Each current pulse resulted in a frequency scan covering ~ 2 cm^{-1}. Absorption in air was detected in a 100 m multipass cell at a reduced pressure of 20-40 Torr. A "zero-air" background subtraction technique[44] was used in order to suppress the influence of H_2O and CO_2 interference effects. Spectra of ambient air and pollutant-free "zero air" were acquired alternatively. The zero-air signal (as a function of a data point number) was subtracted from the ambient air sample signal and normalized to the zero-air signal. This procedure resulted in an absorption spectrum of the ambient air sample. In most measurements, pure air with an addition of 5 % CO_2 was used as the so-called "zero-air" gas.

A typical absorption spectrum of ambient air is shown in Fig. 4. Four strong methane lines, two strong nitrous oxide lines and several water lines corresponding to different isotopic species fall into the spectral range covered by a frequency scan of 2 cm^{-1} centered at 1260 cm^{-1}. The spectrum depicted is the result of averaging over 6,000 individual scans for both ambient air and zero-air. The acquisition and averaging of 6,000 200 μs-long scans with 50 Megasamples per second at 1 kHz repetition rate required ~ 30 seconds. Optimized software could permit faster data acquisition by utilizing a larger fraction of the current pulses.[45] The CH_4 and N_2O concentration levels present in the ambient air were determined by fitting the envelopes of the stronger absorption lines with a Voigt function. The area under a fitting curve was compared with that predicted from the HITRAN database. A detection limit of 2.5 ppbv for CH_4 and 1.0 ppbv for N_2O was determined.

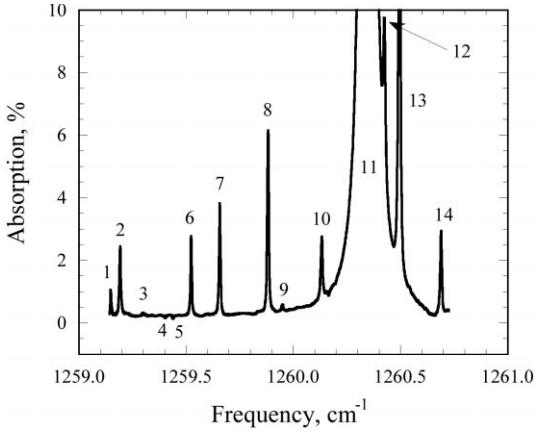

Fig. 4 An example of an absorption spectrum of room air obtained with a cw cryogenically cooled DFB-QC laser based gas sensor. The assignment of the stronger spectral lines is shown: $H_2{}^{16}O$ - 1, 11, 13; N_2O - 2, 3, 10; CH_4 - 6, 7, 8, 14; $H_2{}^{18}O$ - 9; HDO - 12; and CO_2 in the reference zero-air that appears as a negative absorption - 4, 5.

Detection of more complex organic molecules with congested unresolved rotational-vibrational spectra sets a spectroscopic challenge. Traditionally the spectral recognition of such species is performed by acquiring medium-resolution absorption spectra in a wide spectral region and then identifying absorption bands rather than isolated lines. This approach cannot be realized with DFB-QC lasers because of their limited wavelength tunability. However, some molecules present an intermediate case; namely, while the individual optical transitions are not resolved, there is still a sufficiently structured absorption spectrum allowing recognition of the species. The feasibility to detect and quantify such volatile organic compounds (VOCs) was investigated in Ref. 31 using ethanol (C_2H_5OH) as an example.

2.2.2 Nitric oxide detection using widely tunable external cavity QC laser at ~ 5.2 μm

An external cavity (EC) quantum cascade laser configuration with a thermoelectrically cooled gain medium fabricated using a bound-to-continuum design and operating in continuous wave at ~ 5.2 μm was realized in 2005.[26] The EC-QCL architecture as depicted in Fig. 5 employs a piezo-activated cavity mode tracking system for mode-hop free operation suitable for high resolution spectroscopic applications and multiple species trace-gas detection. The performance of the EC-QCL exhibits coarse single mode tuning over 35 cm^{-1} and a continuous mode-hop free fine tuning range of ~ 1.2 cm^{-1} shown in Fig. 6.

3. Trace gas detection based on photoacoustic spectroscopy using QC and IC lasers

Photoacoustic spectroscopy (PAS), based on the photoacoustic effect, in which acoustic waves result from the absorption of laser radiation by a selected target compound in a specially designed cell is another effective method for sensitive trace gas

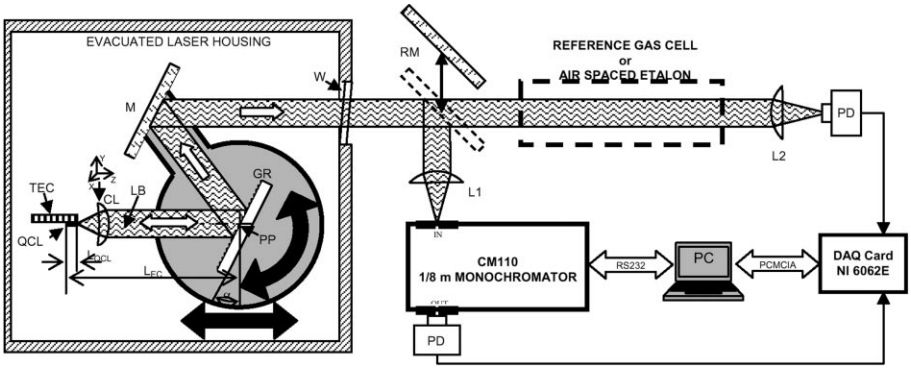

Fig. 5 Schematic diagram of the EC QCL laser and the associated measurement system. QCL – quantum cascade laser, TEC – thermoelectric cooler, CL –collimating lens (1'' diameter, f/0.6, Ge AR-coated 3-12 μm) mounted on a motorized 3D translation stage, LB –laser beam, GR – diffraction grating (150 gr/mm blazed for 5.4 μm), PP – pivot point of the rotational movement, M – mirror (mounted on the same platform with GR), W – CaF_2 window (thickness 4mm, tilted ~ 5 °), RM – removable mirror, PD –photodetector (Hg-Cd-Zn-Te, TE-cooled, Vigo Systems, PDI-2TE-6), L1, L2 – ZnSe lenses.

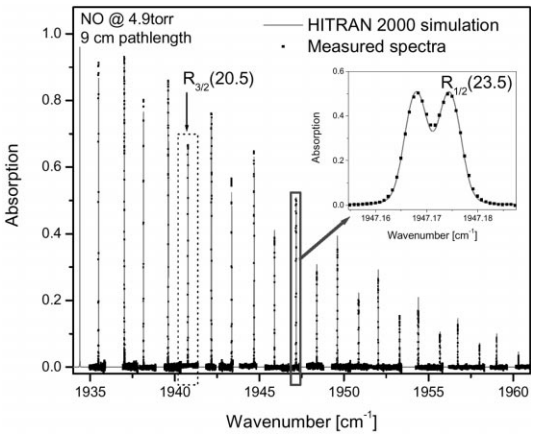

Fig. 6 Nitric oxide absorption spectra measured at different diffraction grating angles of the external cavity quantum cascade laser. The narrow laser linewidth allows resolving two spectral peaks separated by ~ 0.006 cm^{-1} (see inset).

detection. In contrast to other mid-IR absorption techniques, PAS is an indirect technique in which the effect on the absorbing medium and not the direct light absorption is detected. Light absorption results in a transient temperature effect, which then translates into kinetic energy or pressure variations in the absorbing medium via non-radiative relaxation processes that can be detected with a sensitive microphone. PAS is ideally a background-free technique, since the signal is generated by the absorbing gas. In real PAS experiments background signals can originate from nonselective absorption of the gas cell windows (coherent noise) and an outside acoustic (incoherent) noise. PAS signals are proportional to the pump laser intensity and therefore PAS is most effective with high-power laser excitation. A sensitivity of 8 ppmv was demonstrated with only 2 mW of modulated diode laser power in the CH_4 overtone region.[46] The implementation of DFB- QC laser excitation in the fundamental absorption region has the potential of considerably improved sensitivity.

3.1 Photoacoustic spectroscopic techniques

In 2001, D. Hofstetter et al.[47,48] reported PAS measurements of ammonia, methanol and carbon dioxide using a pulsed QC-DFB laser operated at 3-4 % duty cycle with 25 ns long current pulses (2 mW average power) and close to room temperature with Peltier cooling. Temperature tuning resulted in a wavelength range of 3 cm^{-1} with a linewidth of 0.2 cm^{-1}. This sensor used a 42 cm long PAS cell with a radial 16-microphone array for increased detection sensitivity. In addition the cell was placed between two concave reflectors resulting in 36 passes through the cell (with an effective pathlength of 15 m). The laser beam was mechanically chopped at a resonant cell frequency of 1.25 kHz, which resulted in PAS signal enhancement by a Q factor of 70 l. Detection of ammonia concentrations at the 300 ppbv level with a SNR of 3 was achieved at a pressure of 300 Torr.

Ammonia and water vapor photoacoustic spectra were obtained using a cw cryogenically cooled QC-DFB laser with a 16 mW power output at 8.5 microns as reported in Ref. 49. A PAS cell resonant at 1.66 kHz was used. Measured concentrations ranged from 2,200 ppmv to 100 ppbv. The microphone PAS signal was processed by a lock-in amplifier and normalized to the intensity measured by a HgCdTe detector. A detection limit of 100 ppbV ammonia (~ 10^{-5} noise-equivalent absorbance) at standard temperature and pressure was obtained for a 1 Hz bandwidth and a measurement interval of 10 min. Hence the sensitivity obtained is comparable with that achieved by the direct absorption techniques described in section 2, but the required scan times are longer in this PAS study.

3.2 Quartz enhanced photoacoustic spectroscopic techniques

A recently introduced novel approach to photoacoustic detection of trace gases utilizing a quartz tuning fork (QTF) as a sharply resonant acoustic transducer was first reported in 2002.[50,51] Advantages of the technique called quartz-enhanced photoacoustic spectroscopy (QEPAS) compared to conventional resonant photoacoustic spectroscopy include QEPAS sensor immunity to environmental acoustic noise, a simple absorption detection module design, and its capability to analyze small gas samples, down to 1 mm^3 in volume. The measured normalized noise equivalent absorption coefficient for H_2O is 1.9×10^{-9} cm^{-1} W/ $Hz^{-1/2}$ in the overtone region at 7306.75 cm^{-1} is the best among the tested trace gas species to date indicative of fast vibrational-translational relaxation of initially excited states.[50] An experimental study of the long-term stability of a QEPAS-based ammonia sensor indicated that the sensor exhibits very low drift, which allows data averaging over > 3 hours of continuous concentration measurements.

3.2.1 Formaldehyde detection using an interband cascade laser at 3.53 μm

A novel continuous-wave mid-infrared distributed feedback interband cascade laser was utilized to detect and quantify formaldehyde (H_2CO) using quartz enhanced photoacoustic spectroscopy.[52] The sensor architecture is depicted in Fig. 7. The laser was operated at liquid-nitrogen temperatures and provided a single-mode output power of up to 12 mW at 3.53 μm (2832.5 cm^{-1}). The noise equivalent (1σ) detection sensitivity of the sensor was measured to be 1.1×10^{-8} $cm^{-1}W/Hz^{-1/2}$ for H_2CO in ambient air, which corresponds to a detection limit of 0.28 ppmv for a 1 s sensor time constant and 4.6 mW laser power delivered to the absorption detection module.

4. Sensors using a high-finesse optical cavity

Sensitive laser absorption spectroscopy often requires a long effective pathlength of the probing laser beam in media being analyzed. Traditionally, this requirement is satisfied using an optical multipass cell as described in section 2. Such an approach has a number of shortcomings, especially for compact gas sensors. Multipass cells tend to be bulky requiring a large footprint. For example, a commercial 100 m pathlength multipass cell (offered by Aerodyne, Inc.) has a volume of 3.5 liters. Such gas absorption cells also require costly large-aperture mirrors sometimes with aspheric surfaces. An alternative way to obtain a long optical path is to make the light bounce along the same path between two parallel ultralow-loss dielectric mirrors. An effective optical pathlength of several kilometers can be obtained in a very small volume. The light leaking out of such an optical cavity can be used to characterize the absorption of the intracavity medium. Presently a variety of techniques exists to perform high-sensitivity absorption spectroscopy in a high finesse optical cavity (for example, see Ref. 17). One of the most advanced method is the so-called "Noise-Immune Cavity-Enhanced Optical Heterodyne Spectroscopy" (NICE-OHMS) technique.[53] It has the potential to provide shot-noise limited sensitivity with an effective pathlength determined by the cavity ringdown time. The first implementations of this technique in combination with a DFB-QC laser is reported in Ref. 54. However, this approach is technically sophisticated and therefore not suitable for most practical chemical-sensing applications. Two simpler methods are cavity ringdown spectroscopy (CRDS) and integrated cavity output spectroscopy (ICOS).

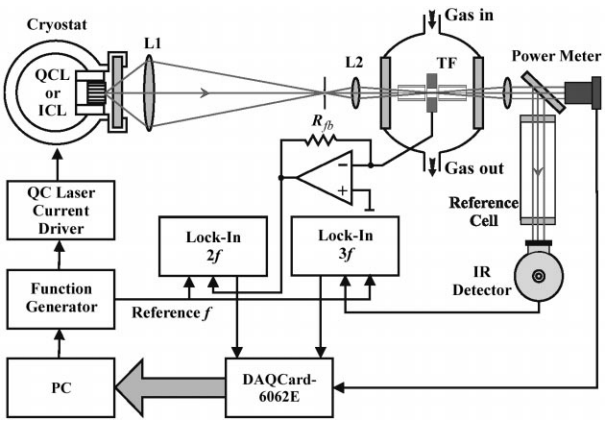

Fig. 7 Schematic of a QCL or ICL based QEPAS sensor platform.

4.1 Cavity ringdown spectroscopy

The first CRDS measurements with a QC-DFB laser were reported in 2000.[55] The authors used a cw laser generating 16 mW at $\lambda = 8.5$ μm. The measured ringdown time of the empty three-mirror cavity was 0.93 μs. An acousto-optic modulator was used to interrupt the cavity injection for ringdown time measurements. The system was tested on diluted NH_3 mixtures. A noise-equivalent sensitivity of 0.25 ppbv and an estimated 1.0×10^{-9} cm^{-1} detectable absorbance limit were reported.

4.1.1 NO detection using CRDS at 5.2 μm

NO is the major oxide of nitrogen formed during high-temperature combustion as well as an important nitrogen-containing species in the atmosphere (NO is a precursor of smog and acid rain) as mentioned in sub-section 2.1.3. NO is also involved in a number of vital physiological processes, and its detection in exhaled breath has potential applications (e.g. as a biomarker for a number of lung diseases like lower-airway inflammation or asthma) in noninvasive medical diagnostics.

A spectroscopic gas sensor for nitric oxide detection based on a cavity ringdown technique was reported in Ref. 56. A cw quantum-cascade distributed-feedback laser operating at 5.2 μm was used as a tunable single-frequency light source. Both laser-frequency tuning and abrupt interruptions of the laser radiation were performed by manipulation of the laser current. A single ringdown event sensitivity to absorption of 2.2×10^{-8} cm^{-1} was achieved. Concentration measurements of ppbv levels of NO in N_2 with a 0.7-ppb standard error for a data collection time of 8 s was achieved.

4.2 Cavity enhanced absorption spectroscopy

A gas analyzer based on a continuous-wave mid-IR quantum cascade laser operating at ~ 5.2 μm and on off-axis integrated cavity output spectroscopy (ICOS) has been developed to measure NO concentrations in human breath.[57] A compact sample cell, 5.3 cm in length and with a volume of ~ 80 cm^3, which is suitable for on-line and off-line measurements during a single breath cycle, was designed and tested. A noise-equivalent (signal-to-noise ratio of 1) sensitivity of 10 ppbv of NO was achieved. The combination of ICOS with wavelength modulation resulted in a 2-ppbv noise-equivalent sensitivity. The total data acquisition and averaging time was 15 s in both cases.

In 2005 a nitric oxide sensor based on a thermoelectrically cooled, cw DFB QCL laser operating at 5.45 μm (1835 cm^{-1}) and off-axis ICOS combined with a wavelength-modulation technique was developed to determine NO concentrations at the sub-ppbv levels that are essential for a number of applications, such as medical diagnostics (specifically in detecting NO in exhaled human breath) and environmental monitoring, The sensor employs a 50-cm-long high-finesse optical cavity that provides an effective path length of 700 m. A noise equivalent minimum detection limit of 0.7 ppbv with a 1-s observation time was achieved.[58]

5. Conclusions

Progress to-date in terms of performance optimization of various cw and pulsed single frequency QC and IC laser based trace gas sensors that use different sensitivity enhancement schemes and achieve minimum detectable absorbances (10^{-4} to 10^{-6}) limited by laser, optical and detector noise sources have been described. Compact, sensitive, and selective gas sensors based on

mid-infrared QCLs and ICLs have been demonstrated to be effective in numerous applications since 1998. These now include such diverse fields as environmental monitoring (e.g. CO, CO_2, CH_4 and H_2CO which are important C_y gases in global warming and ozone depletion studies), industrial emission measurements (e.g. fence line perimeter monitoring in the petrochemical industry, combustion sites, waste incinerators, down gas well monitoring, gas pipeline and compressor station safety), urban (e.g. automobile traffic, power generation) and rural emissions (e.g. horticultural greenhouses, fruit storage and rice agro-ecosystems), chemical analysis and control for manufacturing processes (e.g. semiconductor, pharmaceutical, food), detection of medically important molecules (e.g. NO, CO, CO_2, NH_3, C_2H_6 and CS_2), toxic gases, drugs, and explosives relevant to law enforcement and public safety, and spacecraft habitat air-quality and planetary atmospheric science (e.g. such planetary gases as H_2O, CH_4, CO, CO_2 and C_2H_2).

To date, QC laser-based chemical sensors primarily use InGaAs/InAlAs type-I QC-DFB devices. There are two limitations inherent to this kind of lasers for chemical sensing. First, they cannot access the spectral region of C-H, O-H and N-H stretch vibrations near 3000 cm^{-1}. This shortcoming can be overcome by developing QC lasers based on alternative materials and structures. For example, the 3000 cm^{-1} region is accessible by IC lasers or integrated parametric frequency converted type I QCL structures. Another issue is the limited wavelength tunability of each QC-DFB laser, which restricts the feasibility of probing the entire molecular absorption spectrum, especially of volatile organic compounds and hydrocarbons as well as multicomponent chemical sensing. This requirement can be addressed by separating the gain medium from the wavelength-selective element. In Ref. 26 a QC laser tunability of ~ 35 cm^{-1} at a fixed temperature was demonstrated in an external cavity configuration with a diffraction grating. This is ~ ten times wider range than typically achieved for DFB-QC lasers by means of current tuning. In 2002 an ultra-broadband laser medium based on a number of combined dissimilar intersubband optical transitions was reported.[59] This medium can provide optical gain from 5 to 8 microns wavelength, which corresponds to a potential QC gain bandwidth of > 400 cm^{-1}.

Acknowledgments

The authors thank Dr. Robert F. Curl for numerous useful discussions and support of this work. We are also grateful to Drs. C. Gmachl, F. Capasso, J Faist and R. Yang for their invaluable scientific support. Financial support of the research performed by the Rice group was provided by the National Aeronautics and Space Administration via awards from the Johnson Space Center, Houston, TX and JPL, Pasadena, CA, the Pacific Northwest National Laboratory, Office of Naval Research via a subaward of Texas A & M University, the Texas Advanced Technology Program, the National Science Foundation and the Welch Foundation.

References

1) F. K. Tittel, D. Richter, and A. Fried: *Solid State Mid-Infrared Laser Sources*, I. T Sorokina, and K. L. Vodopyanov (Eds), Springer Verlag, Topics Appl. Phys. **89** (2003) p. 445.
2) R. F. Curl and F. K. Tittel: Ann. Rep. Prog. Chem., Sect. C **98** (2002) 219.
3) T. Yanagawa, H. Kanbara, O. Tadanaga, M. Asobe, H. Suzuki, and J. Yumoto: Appl. Phys. Lett. **86** (2005) 161106.
4) D. Richter and P. Weibring: Appl. Phys. B **82** (2006) 479.
5) A. A. Kosterev and F. K. Tittel: IEEE JQE Special Issue on QC Lasers **38** (2002) 582.
6) F. Capasso, C. Gmachl, R. Paiella, A. Tredicucci, A. L. Hutchinson, D. L. Sivco, J. N. Baillargeon, and A. Y. Cho: IEEE Selected Topics in Quantum Electronics **6** (2000) 931, and references therein.
7) J. Faist, D. Hofstetter, M. Beck, T. Aellen, M. Rochat, and S. Blaser: IEEE Journal of Quantum Electronics **38** (2002) 533.
8) M. Beck, D. Hofstetter, T. Aellen, J. Faist, U. Oesterle, M. Ilegems, E. Gini, and H. Melchior: Science **295** (2002) 301.
9) Ch. Mann, Q. K. Yang, F. Fuchs, W. Bronner, R. Kiefer, K. Koehler, H. Schneider, R. Kormann, H. Fischer, T. Gensty, and W. Elsaesser: B. Adv. in Solid State Phys. Kramer (Ed.), Springer Verlag **43** (2003) 351.
10) A. Evans, J. S. Yu, S. Slivken, and M. Razeghi: Appl. Phys. Lett. **85** (2004) 2166.
11) M. Troccoli, D. Bour, S. Corzine, G. Hofler, A. Tandon, D. Mars, D. J. Smith, L. Diehl, and F. Capasso: Appl. Phys. Lett. **85** (2004) 5842.
12) R. Q. Yang, J. L Bradshaw, J. D. Bruno, J. T. Pham, and D. E. Wortman: IEEE J. Quantum Electron. **38** (2002) 547.
13) R. Q Yang , C. J. Hill, B. H. Yang, C. M. Wong, R. E. Muller, and P. M. Echternach: Appl. Phys. Lett. **84** (2004) 3699.
14) J. L. Bradshaw, N. P. Breznay, J. D. Bruno, J. M. Gomes, J. T. Pham, F. J. Towner, D. E. Wortman, R. L. Tober, C. J. Monroy, and K. A. Olver: Physica E **20** (2004) 479.
15) L. Hvozdara, S. Gianordoli, G. Strasser, W. Schrenk, K. Unterrainer, E. Gornik, C. S. S. S. Murthy, M. Kraft, V. Pustogow, B. Mizaikoff, A. Inberg, and N. Croitoru: Appl. Opt. **39** (2000) 6926.
16) C. Sirtori, H. Page, C. Becker, and V. Ortiz: IEEE J. Quantum Electron. **38** (2002) 559.
17) G. Berden, R. Peeters, and G. Meijer: Int. Reviews in Phys. Chemistry **19** (2000) 565.
18) C. R. Webster, G. J. Flesch, D. C. Scott, J. E. Swanson, R. D. May, W. S. Woodward, C. Gmachl, F. Capasso, D. L. Sivco, J. N. Baillargeon, A. L. Hutchinson, and A. Y. Cho: Appl. Opt. **40** (2001) 321.
19) T. L. Myers, R. M. Williams, M. S. Taubman, F. Capasso, C. Gmachl, D. L. Sivco, J. N. Baillargeon, and A. Y Cho: Opt. Lett. **27** (2002) 170.
20) M. S. Taubmann, T. L. Myers, B. D. Cannon, R. M. Wiliams, F. Capasso, C. Gmachl, D. L. Sivco, and A. Y. Cho: Opt. Lett. **27** (2002) 2164.
21) K. Namjou, S. Cai, E. A. Whittaker, J. Faist, C. Gmachl, F. Capasso, D. L. Sivco, and A. Y. Cho: Opt. Lett. **23** (1998) 219.
22) D. Hofstetter, M. Beck, T. Aellen, J. Faist, U. Oesterle, M. Ilegems, E. Gini, and H. Melchior: Appl. Phys. Lett. **78** (2001) 1964.
23) D. Weidmann, F. K. Tittel, T. Aellen, M. Beck, D. Hofstetter, J. Faist, and S. Blaser: Appl. Phys. **79** (2004) 907.
24) C. Peng, G. Luo, and H. Q. Le: Appl. Opt. **42** (2003) 4877.
25) R. Maulini, M. Beck, and J. Faist: Appl. Phys. Lett. **84** (2004) 1659.
26) G. Wysocki, R. F. Curl, F. K. Tittel, R. Maulini, J. M. Bulliard, and J. Faist: Appl. Phys. B **81** (2005) 769.
27) A. A. Kosterev, F. K. Tittel, C. Gmachl, F. Capasso, D. L. Sivco, J. N. Baillargeon, A. L. Hutchinson, and A. Y. Cho: Appl. Opt.-LP **39** (2000) 6866.
28) D. M. Sonnenfroh, W. T. Rawlins, M. G. Allen, C. Gmachl, F. Capasso, A. L. Hutchinson, D. L. Sivco, J. N. Baillargeon, and A. Y. Cho: Appl. Opt. **40** (2000) 812.
29) E. Normand, M. McCulloch, G. Duxbury, and N. Langford: Opt. Lett. **28** (2003) 16.
30) M. T. McCulloch, E. L. Normand, N. Langford, G. Duxbury, and D. A. Newham: J. Opt. Soc. Am **20** (2003) 1761.
31) A. A. Kosterev, R. F. Curl, F. K. Tittel, C. Gmachl, F. Capasso, D. L. Sivco, J. N. Baillargeon, A. L. Hutchinson, and A. Y. Cho: Appl. Opt. **39** (2000) 4425.
32) D. Weidmann, G. Wysocki, C. Oppenheimer, and F. K. Tittel: Appl. Phys. B **80** (2005) 255.
33) A. A Kosterev, R. F. Curl, F. K. Tittel, R. Kochler, C. Gmachl, F. Capasso, D. L. Sivco, A. Y. Cho, S. Wehe, and M. Allen: Appl. Opt. **41** (2002) 1169.
34) L. S. Rothman, A. Barbe, D. Chris Benner, L. R. Brown, C. Camy-Peyret, M. R. Carleer, K. Chance, C. Clerbaux, V. Dana, V. M. Devi, A. Fayt, J. M. Flaud, R. R. Gamache, A. Goldman, D. Jacquemart,

K. W. Jucks, W. J. Lafferty, J. Y. Mandin, S. T. Massie, V. Nemtchinov, D. A. Newnham, A. Perrin, C. P. Rinsland, J. Schroeder, K. M. Smith, M. A. H. Smith, K. Tang, R. A. Toth, J. Vander Auwera, P. Varanasi, and K. Yoshino: J. Quant. Spectrosc. Radiat. Transfer **82** (2003) 5.
35) A. A. Kosterev, R. F. Curl, F. K. Tittel, R. Köhler, C. Gmachl, F. Capasso, D. L. Sivco, and A. Y. Cho: Applied Optics **41** (2002) 573.
36) G. R. Price, K. K. Botros, and G. M. Goldin: Journal of Engineering for Gas Turbines and Power **124** (2002) 276.
37) C. Stroud, S. Madronich, E. Atlas, B. Ridley, F. Flocke, A. Weinheimer, B. Talbot, A. Fried, B. Wert, R. Shetter, B. Lefer, M. Coffey, B. Heikes, and D. Blake: Atmospheric Environment **37** (2003) 3351.
38) P. E. Silkoff, M. Caramori, L. Tremblay, P. McClean, C. Chaparro, S. Kesten, M. Hutcheon, A. S. Slutsky, N. Zamel, and S. Keshavjee: American Journal of Respiratory and Critical Care Medicine **157** (1998) 1822.
39) S. A. Kharitonov and P. J. Barnes: American Journal of Respiratory and Critical Care Medicine **163** (2001) 1693.
40) G. Wysocki, A. A. Kosterev, and F. K. Tittel: Appl. Phys. B **80** (2005) 617.
41) D. D. Nelson, J. H. Shorter, J. B. McManus, and M. S. Zahniser: Appl. Phys. B **75** (2002) 343.
42) S. W. Sharpe, J. F. Kelly, J. S. Hartman, C. Gmachl, F. Capasso, D. L. Sivco, J. N. Baillargeon, and A. Y. Cho: Opt. Lett. **23** (1998) 1396.
43) A. A. Kosterev, R. F. Curl, F. K. Tittel, C. Gmachl, F. Capasso, D. L. Sivco, J. N. Baillargeon, A. L. Hutchinson, and A. Y. Cho: Opt. Lett. **24** (1999) 1762.
44) A. Fried, S. Sewell, B. Henry, B. P. Wert, T. Gilpin, and J. R. Drummond: J. Geophys. Res. **102** (1997) 6253.
45) D. D. Nelson, B. McManus, S. Urbanski, S. Herndon, and M. S. Zahniser: Spectrochimica Acta A **60** (2004) 3325.
46) G.-C. Liang, H.-H. Liu, A. H. Kung, A. Mohacsi, A. Miklos, and P. Hess: J. Phys. Chem. Av. **104** (2000) 10179.
47) D. Hofstetter, M. Beck, J. Faist, M. Naegele, and M. W. Sigrist: Opt. Lett. **26** (2001) 887.
48) M. Nägele, D. Hofstetter, J. Faist, and M. W. Sigrist: Analytical Sciences **17** Special Issue (2001) s497.
49) B. A. Paldus, T. G. Spence, R. N. Zare, J. Oomens, F. J. M. Harren, D. H. Parker, C. Gmachl, F. Capasso, D. L. Sivco, J. N. Baillargeon, A. L. Hutchinson, and A. Y. Cho: Opt. Lett. **24** (1999) 178.
50) A. A. Kosterev, Y. A. Bakhirkin, R. F. Curl, and F. K. Tittel: Opt. Lett. **27** (2002) 1902.
51) A. A. Kosterev, F. K. Tittel, D. Serebryakov, A. Malinovsky, and A. Morozov: J. Sci. Instrum. Rev. **76** (2005) 043105.
52) M. Horstjann, Y. A. Bakhirkin, A. A. Kosterev, R. F. Curl, and F. K. Tittel: Appl. Phys. B **79** (2004) 799.
53) J. Ye, L.-S. Ma, and J. L. Hall: Opt. Let. **21** (1996) 1000.
54) M. S. Taubman, R. M. Williams, T. L. Myers, F. Capasso, C. Gmachl, D. L. Sivco, A. L. Hutchinson, and A. Y. Cho: Conference on Lasers and Electro-Optics (CLEO 2002), Long Beach, CA, May 19-24, 2002.
55) B. A. Paldus, C. C. Harb, T. G. Spence, R. N. Zare, C. Gmachl, F. Capasso, D. L. Sivco, J. N. Baillargeon, A. L. Hutchinson, and A. Y. Cho: Opt. Lett. **25** (2000) 666.
56) A. A Kosterev, A. A. Malinovsky, F. K. Tittel, C. Gmachl, F. Capasso, D. L. Sivco, J. N. Baillargeon, A. L. Hutchinson, and A. Y. Cho: Appl. Opt. **40** (2001) 5522.
57) Yu. A. Bakhirkin, A. A. Kosterev, C. Roller, R. F. Curl, and F. K. Tittel: Appl. Opt. **43** (2004) 2257.
58) Yu. A. Bakhirkin, A. A. Kosterev, R. Curl, F. K. Tittel, D. A. Yarekha, L. Hvozdara, M. Giovannini, and J. Faist: Appl. Phys. B **82** (2006) 149.
59) C. Gmachl, D. L. Sivco, R. Colombelli, F. Capasso, and A. Y. Cho: Nature **415** (2002) 883.